

NMR Experimental Demonstration of Probabilistic Quantum Cloning

Hongwei Chen^{1,2}, Dawei Lu¹, Bo Chong^{1,3}, Gan Qin¹, Xianyi Zhou¹, Xinhua Peng^{1,*}, and Jiangfeng Du^{1†}

¹*Hefei National Laboratory for Physical Sciences at Microscale and Department of Modern Physics, University of Science and Technology of China, Hefei, Anhui 230026, People's Republic of China.*

²*High Magnetic Field Laboratory, Hefei Institutes of Physical Science, Chinese Academy of Sciences, Hefei 230031, People's Republic of China*

³*College of Science, Xi'an University of Architecture and Technology, Xi'an 710055, P. R. China*

(Dated: June 3, 2018)

The method of quantum cloning is divided into two main categories: approximate and probabilistic quantum cloning. The former method is used to approximate an unknown quantum state deterministically, and the latter can be used to faithfully copy the state probabilistically. So far, many approximate cloning machines have been experimentally demonstrated, but probabilistic cloning remains an experimental challenge, as it requires more complicated networks and a higher level of precision control. In this work, we designed an efficient quantum network with a limited amount of resources, and performed the first experimental demonstration of probabilistic quantum cloning in an NMR quantum computer. In our experiment, the optimal cloning efficiency proposed by Duan and Guo [Phys. Rev. Lett. **80**, 4999 (1998)] is achieved.

PACS numbers: 03.67.-a, 03.67.Dd, 76.60.-k

The no-cloning theorem states that an arbitrary quantum state cannot be cloned perfectly [1]. This is a direct consequence of the linearity of quantum mechanics, and constitutes one of the most fundamental differences between the classical and quantum information theory. Remarkably, this property is also the crucial element for guaranteeing the security of many quantum key distribution protocols. Although quantum states can not be cloned faithfully, in a seminal paper, Bužek and Hillery proposed an "approximate cloning machine" that can produce two identical copies approximately close to the original one [2]. On the other hand, quantum cloning machines are of significant importance in quantum cryptography as they provide the optimal eavesdropping technique for a large class of attacks on many quantum key distribution protocols [3, 4] and have attracted a great deal of interest in further research [5–11]. Up to now, several approximate cloning machines have been experimentally demonstrated in optical systems [12–18] and NMR systems [19–21].

Apart from the idea of an approximate cloning machine, an interesting alternative quantum cloning machine, probabilistic quantum cloning machine (PQCM), was proposed by Duan and Guo [22]. They showed that states randomly chosen from a known set of states can be probabilistically cloned with perfect fidelity, if the states in the set are linearly independent. More specifically, if the states in the set are two non-orthogonal states $|\psi_1\rangle$ and $|\psi_2\rangle$, the *cloning fidelity* will be 1 and the optimal *cloning efficiency* γ is given by $1/(1 + |\langle\psi_1|\psi_2\rangle|)$.

There are many theoretical investigations on PQCM in literatures [23–25], and resource demanding experimental proposals exist [26]. However, to the best of our knowledge, no experiment has been reported until now. To make the experiment feasible, one should overcome two difficulties: (i) to minimize the quantum network com-

plexity, and (ii) to achieve precise quantum control at a certain error threshold. In this work, we successfully solved these two problems and experimentally demonstrated the probabilistic quantum cloning machine with optimal cloning efficiency [22].

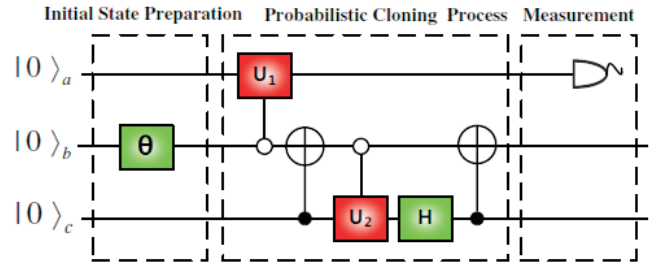


FIG. 1: Quantum logic circuit for the probabilistic quantum cloning demonstration. Qubit a is the probe qubit and qubit c is the clone qubit, they are all initialized in states $|0\rangle$. Qubit b is initially prepared at the to-be-cloned qubit in $|\psi_{in}\rangle_b = |\psi_{\pm\theta}\rangle$ through rotating qubit b by angle $\pm\theta$ around the y -axis. The unitary operation U_1 denotes $R_y(-\alpha)$ and U_2 denotes $R_y(\beta)$, where $\alpha = 2 \arccos(\sqrt{\frac{1+\tan^4 \frac{\theta}{2}}{2}})$ and $\beta = 2 \arccos((\sqrt{\frac{2}{1+\tan^4 \frac{\theta}{2}}} + \sqrt{\frac{2}{1+\tan^{-4} \frac{\theta}{2}}})/2)$.

We start by introducing the experimental scheme to realize the optimal $1 \rightarrow 2$ probabilistic quantum cloning. The quantum logic circuit for the probabilistic quantum cloning process is illustrated in Fig. 1. This is a three-qubit network, which contains one Hadamard gate, two controlled-NOT gates, and two controlled-rotation gates. In this network, qubit a is the probe qubit that indicates whether the cloning progress is successful. Qubit b is the to-be-cloned qubit, which is randomly chosen from the

set $S = \{|\psi_{+\theta}\rangle, |\psi_{-\theta}\rangle\}$, where

$$|\psi_{in}\rangle = |\psi_{\pm\theta}\rangle = \cos\frac{\theta}{2}|0\rangle \pm \sin\frac{\theta}{2}|1\rangle, \quad \theta \in [0, \frac{\pi}{2}]. \quad (1)$$

When $\theta = \pi/2$, the states in the set S are orthogonal. This simplification is reasonable because any pair of arbitrary states $|\psi_1\rangle$ and $|\psi_2\rangle$ can be transformed to the form of Eq. (1) via a unitary rotation. Qubit c is the cloning qubit and initially set to $|0\rangle$. After the unitary evolution, if qubit a is detected in state $|0\rangle$, the cloning process succeeds and we will obtain two perfect copies of the input state $|\psi_{in}\rangle$ at qubit b and c ; and if qubit a is detected in state $|1\rangle$, the cloning process fails.

The output state at the end of the quantum circuit can be written as:

$$\begin{aligned} |\psi_{out}\rangle &= U(|0\rangle|\psi_{in}\rangle|0\rangle) \\ &= \sqrt{\gamma}|0\rangle|\psi_{in}\rangle|\psi_{in}\rangle + \sqrt{1-\gamma}|1\rangle|\Phi\rangle_{BC}, \end{aligned} \quad (2)$$

where U is a unitary operator for the quantum network shown in Fig. 1, the parameter γ is the cloning efficiency and $|\Phi\rangle_{BC} = -\sqrt{1/(1+\tan^4\frac{\theta}{2})}|00\rangle_{BC} - \sqrt{1/(1+\tan^{-4}\frac{\theta}{2})}|11\rangle_{BC}$ is the normalized state of the composite system BC. The first term denotes the success of the $1 \rightarrow 2$ cloning while the second term represents the failure. If we substitute the expressions of the unitary operator U and the input states $|\psi_{in}\rangle$ in Eq. (2), we obtain the cloning efficiency γ as:

$$\gamma(\theta) = \frac{1}{1 + |\langle\psi_{+\theta}|\psi_{-\theta}\rangle|} = \frac{1}{1 + \cos\theta}, \quad (3)$$

which has been proven to be optimal [22, 23]. Compared with the logic circuit of the cloning machine proposed in Ref.[26], this scheme requires fewer quantum logic gates. This setup should be more robust in practice, as it is less affected by experimental imperfections, such as errors in radio-frequency pulses and decoherence.

Using a sample of Diethyl-fluoromalonate, the quantum circuit was implemented on a liquid-state NMR quantum-information processor. Three qubits are represented by the ^1H , ^{13}C and ^{19}F nuclear spins. The molecular structure is shown in Fig.2(a), where the three nuclei used as qubits are marked by the oval. The natural Hamiltonian of three-qubits system in the rotating frame can be written as:

$$H = \sum_{i=a}^c \omega_i I_z^i + 2\pi \sum_{i<j} J_{ij} I_z^i I_z^j, \quad (i, j = a, b, c), \quad (4)$$

where ω_i represent Larmor frequencies, J_{ij} 's are the coupling constants: $J_{ab} = J_{HC} = 161.3$ Hz, $J_{bc} = J_{CF} = -192.2$ Hz and $J_{ac} = J_{HF} = 47.6$ Hz. The experiments were performed at room temperature using a Bruker Avance 400MHz NMR spectrometer equipped with a QXI probe with pulsed field gradient [27, 28].

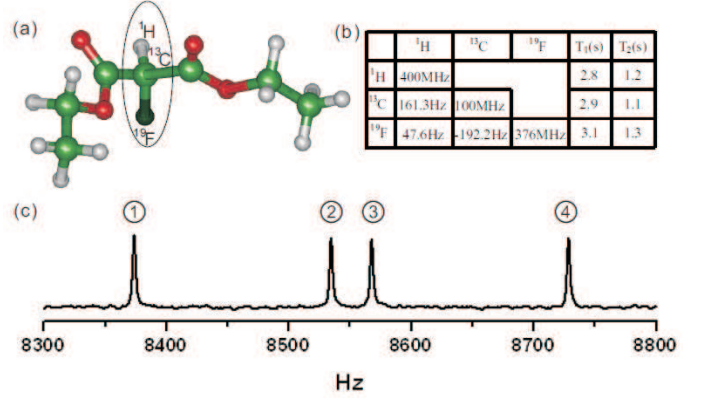


FIG. 2: (color online) Molecular structure, NMR parameters and the ^{13}C equilibrium spectrum of Diethyl-fluoromalonate. (a) Molecular structure of Diethyl-fluoromalonate. Three spin- $\frac{1}{2}$ nuclei as three qubits are marked in oval. (b) The spin-spin couplings and chemical shifts of the three nuclei. (c) The four main peaks in the spectrum corresponding to signal read out from the ^{13}C channel. They respectively correspond to the states $|10\rangle$, $|00\rangle$, $|11\rangle$ and $|01\rangle$ of ^1H and ^{19}F from the left to the right.

The system was first prepared in a pseudo pure state (PPS) $\rho_{000} = \epsilon|000\rangle\langle 000| - \frac{1-\epsilon}{8}I$, where $\epsilon \approx 10^{-5}$ describes the thermal polarization of the system and I is the 8×8 identity matrix, using the method of spatial averaging [29]. From the state ρ_{000} , we prepared the initial state $|0\rangle|\psi_{\pm\theta}\rangle|0\rangle$ through rotating qubit b by angle $\pm\theta$ around the y -axis.

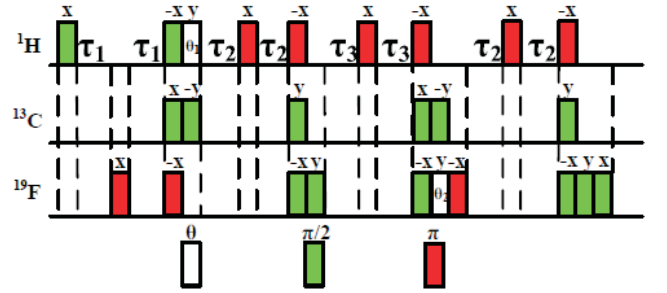


FIG. 3: Pulse sequence for the probabilistic quantum cloning process. The circuit is implemented by hard pulses and free evolutions. The grey rectangles denote $\pi/2$ pulses and the black ones denote the refocusing π pulses. The rectangles labeled with θ_i represent rotations by an angle θ_i , for $\theta_1 = \alpha/2$ and $\theta_2 = (\beta + \pi)/2$. Pulse phases are shown up each pulse. Delay times are $\tau_1 = \frac{\alpha}{4\pi J_{ab}}$, $\tau_2 = \frac{1}{4J_{bc}}$, $\tau_3 = \frac{\beta}{4\pi J_{bc}}$.

The quantum circuit is realized by hard pulses and free evolution. The pulse sequence is depicted in Fig. 3. In principle, the readout procedure should be applied to each of the cloning qubits in the subsequent experiments at the end of the quantum circuit. In this experiment, a sample in natural abundance is used, i.e., only $\approx 1\%$ of the molecules had one ^{13}C nuclear spin. To distin-

guish those molecules from the background molecules, we collect all signals from the cloning qubits through the ^{13}C channel, by applying SWAP gates and measuring the ^{13}C qubit. Figure 2(c) shows the experimental spectra obtained by reading out the ^{13}C qubit. The spectrum consists of four resonance peaks, labeled by the corresponding logical states of the corresponding logical states $|10\rangle$, $|00\rangle$, $|11\rangle$ and $|01\rangle$ of nuclei ^1H and ^{19}F . With respect to the status of probe qubit ^1H , we divide the four signal peaks into two groups: Group 1, including peaks ① and ③, corresponds to state $|1\rangle$ of ^1H , indicating the failure cloning process; and group 2, including peaks ② and ④, corresponds to state $|0\rangle$, indicating the success process. Unlike approximate quantum cloning, the probabilistic cloning machine will yield perfect cloning, and the faulty copies are rejected. In the analysis, we filtered data from group 1, which represents the failing case in the cloning process.

The signal intensity of the initial pseudopure state is measured as the normalized reference. Then the relative signal intensity is measured by digital quadrature detection (DQD). The observable operator can be expressed as $\sigma_x + i\sigma_y$, so the transverse components can be measured as $P_x = \text{Tr}(\rho\sigma_x)$ and $P_y = \text{Tr}(i\rho\sigma_y)$. In the subsequent experiment, the vertical part P_z is measured by applying a $\pi/2$ pulse on the qubit after the cloning process.

It is well-established that probabilistic cloning machine are analyzed with respect to two characteristics: cloning efficiency γ and cloning fidelity F . In the following, we will discuss in details how we can obtain these two parameters from the spectrum data. In the experiment, cloning efficiency γ equals to the population of the probe qubit ^1H in the state $|0\rangle$. It can be measured by comparing the signal intensity of group 2 with the total one, as shown in Eq.(5).

$$\begin{aligned} P_i &= |P_{2i}| + |P_{4i}|, \quad (i = x, y, z) \\ \gamma &= \sqrt{P_x^2 + P_y^2 + P_z^2}. \end{aligned} \quad (5)$$

We have studied the input states as the function of θ , varied from 0 to $\pi/2$ in $\pi/12$ increment. Fig.4 display the average cloning efficiency $\gamma(\theta)$ (green columns) along with the theoretical expectations (red columns). Note that the probabilistic quantum cloning machine can produce faithful copies with probability γ . The cloning efficiency is related to the distinguishable metric of the quantum state space for the input states, since it increases with decreasing of the overlap of the input states in the cloning set S . The result clearly indicates that the larger the overlap between the input states, the smaller the maximum cloning efficiency. As the angle θ approaches $\frac{\pi}{2}$, the cloning efficiency will be close to 1, which is possible if and only if the states are chosen from an orthogonal set.

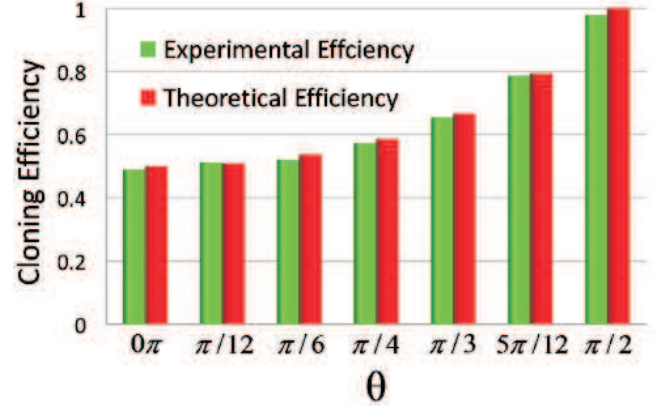


FIG. 4: (Color Online) Experimental efficiencies versus different angles θ of input state. The average experimental efficiencies for each θ are represented at green columns and the red columns corresponding to the optimal values.

After the experimental cloning efficiencies were determined, another important parameters, cloning fidelities, were analyzed. From the Bloch-sphere representation, the state of a single qubit can be represented by a density matrix of the form $\rho = (I + \vec{r} \cdot \vec{\sigma})$, where I is the identity operator and $\vec{\sigma}_\mu$ ($\mu = x, y, z$) are usual Pauli matrices. Let $\rho_0 = |\psi_{in}\rangle\langle\psi_{in}| = \frac{1}{2}(I + \vec{r}_0 \cdot \vec{\sigma})$ be the density matrix for the initial state, while $\rho = \rho_b = \rho_c = \frac{1}{2}(I + \vec{r}_i \cdot \vec{\sigma})$ for the copies. To experimentally determine the fidelities, we need the density operators of the final states of both qubits. The length of the vectors on the Bloch sphere representing the cloned states are found to be $r(\vec{r}_x, \vec{r}_y, \vec{r}_z)$, where $r_i = (P_{2i} + P_{4i})/\gamma$ ($i = x, y, z$). Here, the signal intensity should be divided by γ to compensate the signal loss of faulty copies. The cloning fidelities are expressed as

$$F_i = \text{Tr}(\rho_0 \cdot \rho_i) = \frac{1}{2}(1 + \vec{r}_0 \cdot \vec{r}_i), \quad (i = b, c),$$

For the initial state $|\psi_{in}\rangle = \cos\frac{\theta}{2}|0\rangle \pm \sin\frac{\theta}{2}|1\rangle$, we have $\vec{r}_0 = (\sin(\pm\theta), 0, \cos\theta)$ and the fidelities become

$$F_i = \frac{1}{2}(1 + \sin(\pm\theta) \cdot r_{x_i} + \cos\theta \cdot r_{z_i}). \quad (6)$$

The experimental fidelities of the duplicated states are shown in Fig.5. Fig.5(b)-(d) show the reconstructed density matrices for $\theta = \pi/4$. The vertical axes show the normalized amplitude and the horizontal axes label the basis state in the computational basis. Fig.5(b) represents the matrix for the input state ρ_0 and (c), (d) give the experimental results of ρ_b and ρ_c . The corresponding fidelities are $F_b = 0.99$, $F_c = 0.98$. Fig.5(a) shows the cloning fidelities for the input states $|\psi(\pm\theta)\rangle$ with different angles θ in the cloning set S . In the figure, the cycles denote the cloning fidelities for the second qubit (red) and third qubits (green) for $|\psi(+\theta)\rangle$, while the triangles

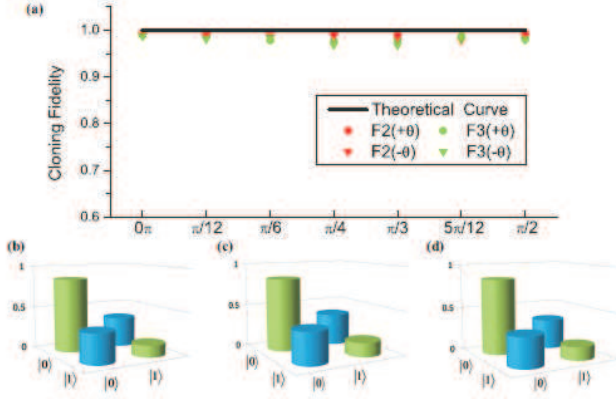


FIG. 5: (color online) Experimental fidelities versus different angles θ of input state. (a) The theoretical values of cloning fidelity are plotted as the solid line. The cycles denote the cloning fidelities for the second qubit (red) and third qubits (green) for $|\psi(+\theta)\rangle$, while the triangles are for $|\psi(-\theta)\rangle$. (b)-(d) show the reconstructed density matrices for $\theta = \pi/4$. (b) represents the matrix for the input state ρ_0 and (c), (d) give the experimental results of ρ_b and ρ_c .

are for $|\psi(-\theta)\rangle$. The average experimental fidelity over different values of θ is about 0.98. The small deviations ($\leq 3\%$) between the experimental and theoretical values are mainly attributed to imperfect calibration of radio frequency pulses. The decoherence from spin relaxation is negligible, since the total experimental time of ~ 8 ms is much shorter than the minimal relaxation time of ~ 1.0 s.

In summary, we have experimentally demonstrated the probabilistic cloning machine in a NMR system by simplifying the network. For two orthogonal states, the cloning machine can always produce two perfect copies with the 100% probability of success. When the original states are non-orthogonal, two faithful copies can be produced with the deterministic probability less than 1. The experimental results are in good agreement with the theoretical prediction, which indicates the cloning network is effective for the all input states. Our experimental scheme can be achieved not only in NMR systems, but also in other physical systems. Further research works in probabilistic cloning, especially in experimental demonstration, will be important for the other quantum information protocols, such as quantum identification, quantum purification and quantum deleting [22, 30, 31].

We thank Prof. J. W. Pan and Dr. W. Harneit for helpful discussions. This work was supported by the National Natural Science Foundation of China, the National Science Foundation for Postdoctoral Scientists, the Fundamental Research Funds for the Central Universities, the CAS, Ministry of Education of PRC, and the National Fundamental Research Program.

[†] Electronic address: djf@ustc.edu.cn

- [1] W. K. Wootters and W. H. Zurek, Nature(London) **299**, 802(1982); D. Dieks, Phys. Lett. **92A**, 271 (1982).
- [2] V. Bužek, and M. Hillery, Phys. Rev. A **54**, 1844(1996).
- [3] C. H. Bennett and G. Brassard, in Proceedings of IEEE International Conference on Computers, Systems and Signal Processing, Bangalore, India (IEEE, New York, 1984), p. 175.
- [4] C.S. Niu and R. B. Griffiths, Phys. Rev. A **60**, 2764 (1999); N. J. Cerf et al., Phys. Rev. Lett. **88**, 127902 (2002); A. Acín, N. Gisin, and V. Scarani, Phys. Rev. A **69**, 012309 (2004).
- [5] V. Scarani, S. Iblisdir, N. Gisin and A. Acín, Rev. Mod. Phys. **77**, 1225(2005).
- [6] N. Gisin, and S. Massar, Phys. Rev. Lett. **79**, 2153 (1997).
- [7] N. J. Cerf, A. Ipe, and X. Rottenberg, Phys. Rev. Lett. **85**, 1754 (2000).
- [8] D. Bruss et al., Phys. Rev. A **62**, 012302 (2000).
- [9] G. M. D'Ariano and P. Lo Presti, Phys. Rev. A **64**, 042308 (2001).
- [10] Y. Delgado, L. Lamata, J. León, D. Salgado and E. Solano, Phys. Rev. Lett. **98**, 150502(2007).
- [11] L. Lamata, J. León, D. Pérez-García, D. Salgado and E. Solano, Phys. Rev. Lett. **101**, 180506(2008).
- [12] Y. F. Huang, et al., Phys. Rev. A **64**, 012315 (2001).
- [13] A. Lamas-Linares et al., Science **296**, 712 (2002).
- [14] F. De Martini, V. Bužek, F. Sciarrino and C. Sias, Nature (London) **419**, 815 (2002).
- [15] S. Fasel, N. Gisin, G. Ribordy, V. Scarani and H. Zbinden, Phys. Rev. Lett. **89**, 107901 (2002).
- [16] Z. Zhao, et al., Phys. Rev. Lett. **95**, 030502 (2005).
- [17] L. Bartuskova, et al., Phys. Rev. Lett. **99**, 120505(2007).
- [18] E. Nagali, L. Sansoni, F. Sciarrino, et al., NATURE PHOTONICS **3**, 720(2009).
- [19] H. K. Cummins, et al. Phys. Rev. Lett. **88**, 187901 (2002).
- [20] J. F. Du, et al., Phys. Rev. Lett. **94**, 040505 (2005).
- [21] H. W. Chen, X. Y. Zhou, Dieter Suter and J. F. Du, Phys. Rev. A **75**, 012317 (2007).
- [22] L. M. Duan and G. C. Guo, Phys. Rev. Lett. **80**, 4999(1998); L. M. Duan and G. C. Guo, Phys. Lett. A **243**, 261(1998).
- [23] A. K. Pati, Phys. Rev. Lett. **83**, 2849(1999).
- [24] D. W. Qiu, J. Phys. A: Math. Gen. **39**, 5135(2006).
- [25] K. Azuma, Phys. Rev. A **72**, 032335 (2005).
- [26] C. W. Zhang, Z. Y. Wang, C. F. Li and G. C. Guo, Phys. Rev. A **61**, 062310(2000); T. Gao et al., e-print arXiv:quant-ph/0308036.
- [27] J. F. Zhang, X. H. Peng, et al. Phys. Rev. Lett. **100**, 100501(2008).
- [28] X. H. Peng, J. F. Zhanget al. Phys. Rev. Lett. **103**, 140501(2009).
- [29] D. G. Cory, M. D. Price and T. F. Havel, Phys. D **120**, 82(1998).
- [30] J. Fiurášek, Phys. Rev. A **70**, 032308 (2004).
- [31] Y. Feng, S. Y. Zhang, and M. S. Ying, Phys. Rev. A. **65**, 042324 (2002).

* Electronic address: xhpeng@ustc.edu.cn